Int J Civ Eng (2017) 15:839–847
DOI 10.1007/s40999-017-0196-5

TECHNICAL NOTE

A Temperature–Age Model For Prediction of Compressive Strength of Chemically Activated High Phosphorus Slag Content Cement

Ali Allahverdi[1,2] · Mostafa Mahinroosta[1] · Shima Pilehvar[1]

Received: 5 October 2015 / Revised: 23 May 2016 / Accepted: 7 June 2016 / Published online: 4 April 2017

Abstract Prediction of compressive strength by a proper model is a fast and cost-effective way for evaluating cement quality under various curing conditions. In this paper, a logarithmic model based on the results of an experimental work conducted to investigate the effects of curing time and temperature on the compressive strength development of chemically activated high phosphorus slag content cement has been presented. This model is in terms of curing time and temperature as independent variables and compressive strength as dependent variable. For this purpose, mortar specimens were prepared from 80 wt.% phosphorus slag, 14 wt.% Portland cement, and 6 wt.% compound chemical activator at Blaine fineness of 303 m^2/kg. The specimens were cured in lime-saturated water under temperatures of 25, 45, 65, 85, and 100 °C in oven. The model has two adjustable parameters for various curing times and temperatures. Modeling has been done by applying dimensionless insight. The proposed model can efficiently predict the compressive strength of this type of high phosphorus slag cement with an average relative error of less than 4%.

Keywords Phosphorous slag · Modeling · Compressive strength · Curing time · Curing temperature

✉ Ali Allahverdi
ali.allahverdi@iust.ac.ir

[1] Research laboratory of Inorganic Chemical Process Technologies, School of Chemical Engineering, Iran University of Science and Technology, Narmak, Tehran 1684613114, Iran

[2] Cement Research Center, School of Chemical Engineering, Iran University of Science and Technology, Narmak, Tehran 1684613114, Iran

List of Symbols

R	Compressive strength (MPa).
R_b	The 28-day compressive strength of Portland cement (MPa).
t	Curing time (day)
t_b	Curing time for nondimensionalization (=28 day).
T	Curing temperature (°C).
T_a	Ambient temperature (K).
T_0	Standard temperature (=0 °C).

Greek Letters

α	The first parameter of the model.
β	The second parameter of the model.
Γ	Dimensionless compressive strength.
α_g	The generalized first parameter of the model.
β_g	The generalized second parameter of the model.
θ	Dimensionless curing temperature.
δ	Dimensionless curing time.

1 Introduction

In addition to being an energy-intensive industry [1], cement industry releases acid gases and also huge volumes of carbon dioxide as a greenhouse gas. These gases in turn cause global warming and acid rain. Therefore, the use of proper materials to replace part of cement can be considered as a suitable way of reducing gas emission. Some types of industrial wastes can fulfill this appropriate goal [2–5]. The use of industrial wastes such as slags (blast furnace slag, phosphorus slag, etc.), fly ash, and silica fume as additives to cement can have several advantages [4–6]: (1) recycling and consequently resource development, (2) helping to reduce environmental pollution, (3) economic benefits, (4) energy savings, and (5) improving the durability

and performance of concrete. Among industrial wastes, only slags exhibit latent cementing property and have attracted the attention of many researchers [4–11].

1.1 Phosphorus Slag

Phosphorus slag (PHS) is an industrial by-product of phosphorus manufacturing industry. The main oxides in the PHS chemical composition are calcium oxide (CaO) and silicon dioxide (SiO_2). The ratio of calcium oxide to silica in the PHS usually alters from 0.8 to 1.2 [7, 8]. PHS has two major weaknesses resulting in its use at low replacement levels as a supplementary cementing material. These two weaknesses are (1) residual phosphorus that impose a significant lag effect on the setting process of Portland cement; and (2) insufficient alumina content that adversely affects the early-age properties [12]. The residual phosphorus is in the form of P_2O_5, which turns into phosphoric acid when comes into contact with water. The pH of the medium, therefore, decreases and this retards the hydration reactions that progress in alkaline environments [7, 8, 13]. The reason for the second weakness is that sufficient alumina in slag results in a higher reactivity at early ages and increases the aluminum incorporation in calcium silicate hydrate (CSH) as one of main hydration products, contributing in compressive strength development [12]. Considering these two weaknesses, it is therefore necessary to apply valid methods that tailor early properties. The most common methods for this purpose are mechanical and/or chemical activations, and thermal treatments including raw material calcinations and/or thermal curing of the product [5, 14]. Present study uses combinations of chemical activation and thermal curing techniques for early-age strength improvement purpose. These two techniques were exerted on high PHS content cement. The prepared cement by these techniques is called chemically activated high phosphorus slag content cement (CAPHSC) [15, 16]. The chemical activation was performed by adding a compound chemical activator. This Portland cement-based activator contains proportioned amounts of different solid chemical activators including anhydrite and sodium sulfate [5, 15–17]. The composition of the chemical activator was adopted from our previous research works [15–17]. The details of the chemical activation and thermal curing are not within the scope of this study. In this work, the main focus is on finding a mathematical model for prediction of compressive strength of CAPHSC. However, it must be noted that this model is not a generalized model for all types of slag-containing cements and it can only be used to predict the compressive strength of CAPHSC, and its applicability for the other types of slag-containing cements needs further investigations.

1.2 Compressive Strength Estimation

The compressive strength of the cement in the set and hardened conditions is the most obviously required value for structural application [18]. Hence, the prediction of compressive strength has been an active area of research and has attracted the attention of many researchers, as far as many efforts have been made to obtain a suitable model which is capable of predicting strength of concrete and mortars at various ages with an acceptable accuracy [19].

The most common modeling techniques for the prediction of cement strength generally include analytical modeling [13, 20, 21], artificial neural network (ANN) [22–27], and statistical methods [28–32].

In mathematical modeling, the use of regression equation is one of the most striking approaches. The most popular regression equation in the prediction of compressive strength is the linear regression [33]:

$$Y = a_0 + a_1X_1 + a_2X_2 + \cdots + a_mX_m, \quad (1)$$

where a_0–a_m, and X_1–X_m are regression coefficients and variables influencing compressive strength, respectively. The above-mentioned equation has been extended by various researchers to include more variables affecting the compressive strength such as fine aggregate-to-cementing material ratio, coarse aggregate-to-cementing material ratio, fineness, curing time, curing temperature, and composition [33]. For example, Chopra et al. [19] earned a multiple regression model in terms of four variables of water-to-cement ratio, fine aggregate-to-cementing material ratio, coarse aggregate-to-cementing material ratio, and cementing material content to predict the compressive strength of concrete with and without fly ash. In another study [33], they used ridge regression as a more reliable method for the prediction of compressive strength of concrete. Tepecik et al. [18] developed multiple linear regression (MLR) models for prediction of the 2-, 7-, and 28-day compressive strength of CEM-I 42.5 using the backward stepwise method. These models are useful to predict the compressive strength of cement when it has various particle sizes and known chemical and mineralogical properties.

According to Eq. (1), all the variables related to the compressive strength are seen in a linear relation, but this is not always true because the variables incorporated in a concrete and mortar mix and affecting their compressive strength are interrelated with each other and this important issue is not observed in Eq. (1). Here, it seems that there is a need to develop another type of mathematical model that can reliably predict the compressive strength of concrete and mortar with acceptably high accuracy. The logarithmic relation can be a proper option as a nonlinear correlation for the multiple dependencies [33]. In our previous study [34], we developed a dimensionless logarithmic model in

Table 1 Chemical composition of phosphorus slag used in this study (wt.%)

SiO_2	Al_2O_3	Fe_2O_3	CaO	MgO	P_2O_5	K_2O	Na_2O	LOI
38.42	7.65	0.90	45.14	2.60	1.50	0.56	0.43	1.87

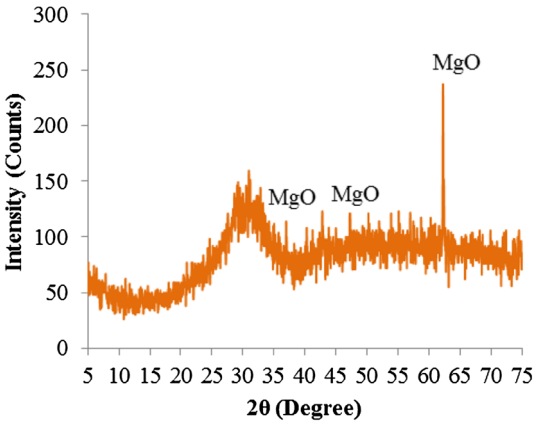

Fig. 1 X-ray diffractogram of phosphorus slag used in this study

terms of water-to cement ratio and curing time to predict the compressive strength of CAPHSC. In the present study, we aim to derive a logarithmic model in terms of curing temperature and time. Two innovative aspects of this model compared to the model proposed in reference [34] are as follows: a model as a function of curing time and temperature is more applicable than a model in terms of curing time and water-to-cement ratio. Also, this model can be used to predict the compressive strength of CAPHSC at curing temperatures higher than ambient temperature.

2 Materials and Methods

2.1 Materials

PHS was provided from a phosphoric acid plant located in Tehran province, Iran. The chemical composition of PHS determined according to ASTM standard C311 is given in Table 1. The density of ground PHS was obtained 2940 kg/m^3 in accordance with ASTM standard C188 using a Le Chatelier flask. Figure 1 depicts the X-ray diffractogram of PHS indicating the presence of periclase (MgO) as the only crystalline phase.

Type II Portland cement (PC) was used in accordance with ASTM standard. The Blaine specific surface area and the specific gravity of PC were 302 and 3120 kg/m^3, respectively. The chemical and Bogue's potential phase compositions of this cement are given in Table 2.

A mixture of sodium sulfate (2 wt.%) and anhydrite (4 wt.%) was used as compound chemical activator. Sodium sulfate used in this study was purchased from Merck (Darmstadt, Germany). The chemical composition of anhydrite (in wt.%) was as follows: CaO-36.00, SO_3-54.38, and SiO_2-5.88.

To prepare specimens, the pipeline potable water was used. The specific gravity of the used water was supposed about 1000 kg/m^3.

2.2 Methods

The inter-grinding of the proportioned mixes of PHS (80 wt%), PC (14 wt.%), and compound chemical activator (6 wt.%) was done using a laboratory single cylinder box ball mill containing spherical steel balls. Its length and diameter were 0.30 and 0.26 m, respectively. The inter-grinding lasted for a period of 7 h until the desired Blaine fineness of 303 m^2/kg was achieved.

The value of Blaine specific surface area (Blaine fineness) was determined according to ASTM standard C204 using a Blaine air permeability apparatus.

To achieve standard normal consistency in fresh mortar, water-to-cement ratio was obtained according to ASTM standard C230 using flow table test. For this test, PC mortar of normal consistency was used as reference. Water-to-cement ratio for PC mortar was 0.485.

AZMOONTEST hydraulic press machine with a capacity of 320 kN was applied for measuring the compressive

Table 2 Chemical and Bogue's potential phase compositions of Type II Portland cement

Chemical composition (wt%)								
CaO	SiO_2	Al_2O_3	Fe_2O_3	MgO	SO_3	K_2O	Na_2O	LOI
63.26	22.50	4.15	3.44	3.25	1.80	0.65	0.20	0.61
Bogue's potential phase composition (wt%)								
C_3S		C_2S		C_3A			C_4AF	
45.62		30.16		5.18			10.47	

(C = CaO, S = SiO_2, A = Al_2O_3, F = Fe_2O_3)

strength of CAPHSC mortar specimens. For each measurement, three cubic specimens of the size 5×5×5 cm were used and the average of three measured values was reported as the result.

Hydrothermal curing was applied to investigate the effects of curing time and temperature on compressive strength development of CAPHSC. The hydrothermal curing of CAPHSC mortar specimens was done at atmospheric pressure using an oven. Various curing regimes were applied in steam-saturated atmosphere at different temperatures of 25, 45, 65, 85, and 100 °C for the purpose of hydrothermal treatments.

The preparation of mortar specimens was performed according to ASTM standard C109. The fresh mortar was cast into 5×5×5 cm molds. After casting, the specimens were precured at an atmosphere of more than 95% relative humidity at 25 °C for the first 24 h, and then after demolding, the hydrothermal curing regimes were followed.

3 Modeling Procedure

In this paper, the modeling approach is based on curve fitting and linear regression. It is better to have a construction route for modeling and follow its steps from the beginning to the end. The route illustrated in Fig. 2 is applied for deriving a prediction model from experimental data.

Experimental results related to the mentioned curing temperatures are given in Table 3. Using these experimental data, a curve fitting is done for each given temperature. It was observed from all curves that compressive strength data follow a general logarithmic equation in the form of $C=\alpha \ln t+\beta$, where C and t are compressive strength (MPa) and curing time (day), respectively. Each curve has its own specific α and β. Finding a model with generalized α and β for all curves will be desirable, and this paper is devoted to find such a model.

3.1 Selection of Variables

Two variables of curing time and temperature are considered as independent variables of modeling. Hereafter, t and T stand for curing time and temperature, respectively. Compressive strength (R) is selected as dependent variable.

3.2 Defining Dimensionless Variables

In this section, dimensionless variables are defined. Nondimensionalization of the variables avoids round-off errors. Dimensionless curing time is obtained by dividing the curing time, t, to t_b. At first, values of 7, 14, and 28 days were allocated to t_b. Later calculations showed that values of 7 and 14 days are not suitable for t_b, because curves plotted with these two values did not have a high correlation factor, R^2, while by assigning the value of 28 days to t_b, all correlation factors were obtained high at about 0.99. Therefore, dimensionless curing time (δ) is calculated using Eq. (2):

$$\delta = t/t_b. \tag{2}$$

Dimensionless curing temperature (θ) is defined according to Eq. (3):

$$\theta = (T + T_0)/T_a, \tag{3}$$

where T_0 (standard temperature) and T_a (ambient temperature) are equal to 273.15 and 298.15 K, respectively. The values of θ are presented in Table 4.

In order to obtain dimensionless compressive strength, it is divided to R_b. The value of R_b is equal to 42.5 MPa. Inasmuch as 28 days was selected for t_b, the 28-day compressive strength of Portland cement, namely 42.5 MPa, was assigned to R_b for better correlation between curing time and compressive strength. So, dimensionless compressive strength (Γ) is defined in accordance with Eq. (4):

$$\Gamma = R/R_b. \tag{4}$$

The values of dimensionless compressive strength for all curing temperatures used in this study are indicated in Tables 5 and 6.

3.3 Finding generalized parameters

As mentioned in Sect. 3, the most important goal of this study is finding adjustable α and β for all curing temperatures used in this work. Such α and β are called the

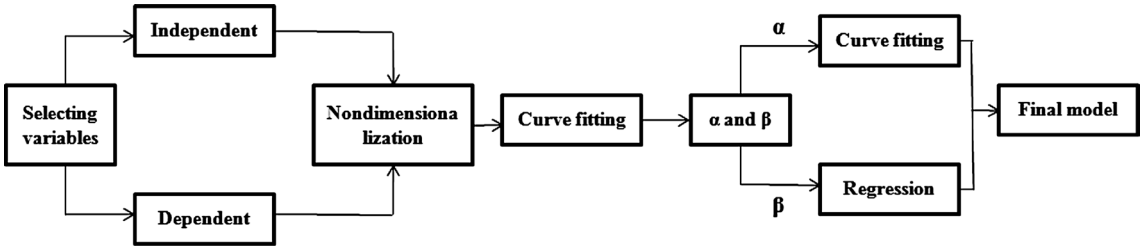

Fig. 2 The construction route used for modeling

Table 3 Experimental data related to curing temperatures used in this study

T (°C)	Compressive strength (MPa)																		
	2 (day)	3 (day)	4 (day)	7 (day)	11 (day)	14 (day)	15 (day)	16 (day)	22 (day)	23 (day)	24 (day)	30 (day)	37 (day)	51 (day)	52 (day)	57 (day)	59 (day)	87 (day)
25	1.25	11.12	14.50	28.80	40.00	46.90	48.51	49.94	57.40	58.38	61.50	64.55	69.43	76.88	77.38	77.62	80.31	87.56
45	34.00	42.25	47.25	57.50	66.20	69.08	70.33	73.00	77.18	80.87	81.78	82.81	88.67	92.30	94.87	95.21	96.20	101.87
65	51.87	57.31	58.65	68.31	72.14	77.69	78.18	79.07	81.30	81.87	82.51	84.75	87.52	89.42	92.80	94.14	94.57	99.65
85	49.00	52.00	55.98	59.75	62.11	63.56	66.60	67.09	68.45	68.65	69.00	69.31	72.14	73.00	76.55	77.31	77.67	80.70
100	40.98	42.71	43.42	46.87	48.75	49.26	50.00	50.82	52.50	52.67	52.87	53.00	54.00	54.75	54.83	55.22	55.37	57.02

Table 4 Values of θ for all curing temperatures used in this study

Curing temperature (°C)	θ
25	1.00
45	1.07
65	1.13
85	1.20
100	1.25

generalized parameters of the model. α_g and β_g stand for the generalized α and β, respectively. By finding these generalized parameters, a model will be achieved that is able to satisfy all data related to curing temperatures under investigation. For the purpose of obtaining parameters, the values of Γ are plotted versus the product of θ and δ, $\theta.\delta$, in a same coordinate system. These plots are depicted in Fig. 3.

The values α and β obtained for each curve shown in Fig. 3 are given in Table 7. Linear regression of the values of α in terms of θ is used to obtain α_g and curve fitting is applied to reach β_g. For β_g, a quadratic equation fitting the values of βversus θ with an acceptable agreement is concluded from curve fitting.

Equations (5) and (6) represent linear function, α_g, and quadratic function, β_g, respectively:

$$\alpha_g = -1.7842\theta + 2.3302, \tag{5}$$

$$\beta_g = -39.2098\theta^2 + 87.1189\theta - 46.4271. \tag{6}$$

Finally, the model for the prediction of compressive strength of CAPHSC is obtained in the form presented in Eq. (7):

$$\Gamma = \alpha_g \ln(\theta.\delta) + \beta_g, \tag{7}$$

in which:

Γ is $R/42.5$
α_g is $-1.7842\theta+2.3302$,
δ is t/t_b
θ is $(T+T_0)/T_a$
β_g is $-39.2098\theta^2+87.1189\theta-46.4271$.

3.4 Model Validation

To verify the validity of the proposed model, a comparison between the experimental results and the results predicted by the proposed model has been carried out. This comparison is shown in Fig. 4. As shown in the figure, the values predicted by the model are very close to experimental data, and this means that the proposed model has a good capability to predict the compressive strength of CAPHSC at different curing temperatures and ages. It should be noted that the proposed model is proper to predict the

Table 5 Dimensionless values of Γ for curing temperature of 25, 45, and 65 °C

t	δ	25 °C			45 °C			65 °C		
		$\theta.\delta$	R	Γ	$\theta.\delta$	R	Γ	$\theta.\delta$	R	Γ
2	0.071	0.071	1.25	0.0294	0.076	34.00	0.8000	0.080	51.87	1.2205
3	0.107	0.107	11.12	0.2616	0.114	42.25	0.9941	0.121	57.31	1.3485
4	0.143	0.143	14.50	0.3411	0.153	47.25	1.1120	0.162	58.65	1.3800
7	0.250	0.250	28.80	0.6776	0.267	57.50	1.3530	0.282	68.31	1.6073
11	0.393	0.393	40.00	0.9412	0.421	66.20	1.5580	0.444	72.14	1.6974
14	0.500	0.500	46.90	1.1035	0.535	69.08	1.6254	0.565	77.69	1.8280
15	0.536	0.536	48.51	1.1414	0.573	70.33	1.6548	0.606	78.18	1.8395
16	0.571	0.571	49.94	1.1751	0.611	73.00	1.7176	0.645	79.07	1.8605
22	0.786	0.786	57.40	1.3506	0.841	77.18	1.8160	0.888	81.30	1.9129
23	0.821	0.821	58.38	1.3736	0.878	80.87	1.9030	0.928	81.87	1.9263
24	0.857	0.857	61.50	1.4470	0.917	81.78	1.9242	0.968	82.51	1.9414
30	1.071	1.071	64.55	1.5188	1.146	82.81	1.9485	1.210	84.75	1.9941
37	1.321	1.321	69.43	1.6336	1.413	88.67	2.0863	1.493	87.52	2.0593
51	1.821	1.821	76.88	1.8089	1.950	92.30	2.1718	2.058	89.42	2.1040
52	1.857	1.857	77.38	1.8207	1.987	94.87	2.2322	2.098	92.80	2.1835
57	2.036	2.036	77.62	1.8263	2.178	95.21	2.2402	2.300	94.14	2.2150
59	2.107	2.107	80.31	1.8896	2.254	96.20	2.2635	2.381	94.57	2.2252
87	3.107	3.107	87.56	2.0602	3.324	101.87	2.3969	3.511	99.65	2.3447

Table 6 Dimensionless values of Γ for curing temperature of 85 and 100 °C

t	δ	85 °C			100 °C		
		$\theta.\delta$	R	Γ	$\theta.\delta$	R	Γ
2	0.071	0.085	49.00	1.1529	0.089	40.98	0.9642
3	0.107	0.129	52.00	1.2235	0.134	42.71	1.0049
4	0.143	0.172	55.98	1.3172	0.179	43.42	1.0216
7	0.250	0.300	59.75	1.4060	0.312	46.87	1.1028
11	0.393	0.472	62.11	1.4614	0.491	48.75	1.1470
14	0.500	0.600	63.56	1.4955	0.625	49.26	1.1590
15	0.536	0.643	66.60	1.5671	0.670	50.00	1.1765
16	0.571	0.685	67.09	1.5786	0.714	50.82	1.1958
22	0.786	0.943	68.45	1.6106	0.982	52.50	1.2353
23	0.821	0.985	68.65	1.6153	1.026	52.67	1.2393
24	0.857	1.030	69.00	1.6235	1.071	52.87	1.2440
30	1.071	1.285	69.31	1.6310	1.339	53.00	1.2470
37	1.321	1.585	72.14	1.6974	1.651	54.00	1.2705
51	1.821	2.185	73.00	1.7176	2.276	54.75	1.2706
52	1.857	2.228	76.55	1.8012	2.321	54.83	1.2901
57	2.036	2.443	77.31	1.8191	2.545	55.22	1.2993
59	2.107	2.530	77.67	1.8275	2.634	55.37	1.3028
87	3.107	3.730	80.70	1.8988	3.884	57.02	1.3416

compressive strength of CAPHSC at the curing ages of more than a day and its applicability for the ages of less than one day (e.g., several hours) needs further investigations. The average errors of the model at each curing temperature are given in Table 8. The model has the maximum error at temperature of 25 °C and the minimum error at 85 °C.

4 Conclusion

A temperature–age model was proposed to predict the compressive strength of chemically activated high phosphorus slag content cement. This model was derived based on curve fitting and linear regression of experimental data. The model has two linear and logarithmic parts,

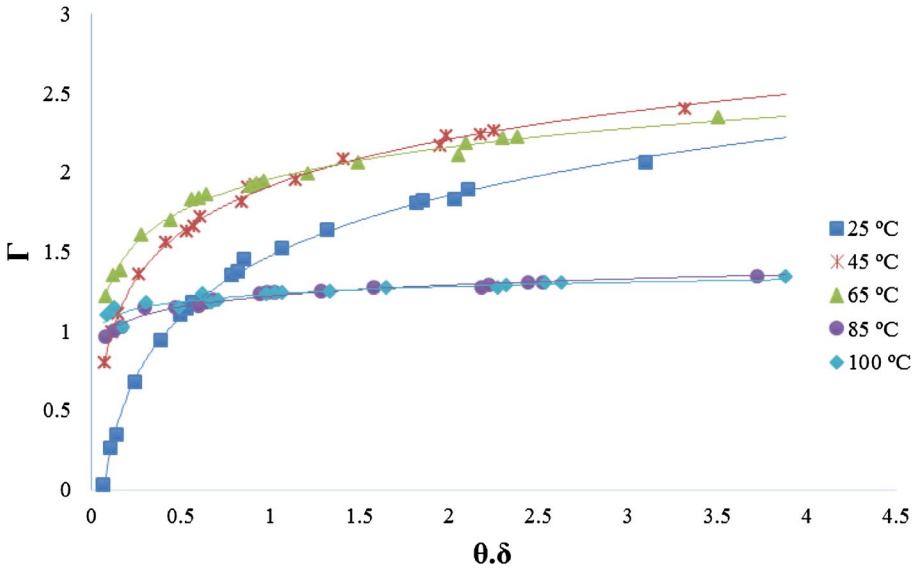

Fig. 3 The plots of Γ versus $\theta.\delta$ for all curing temperatures used in this study

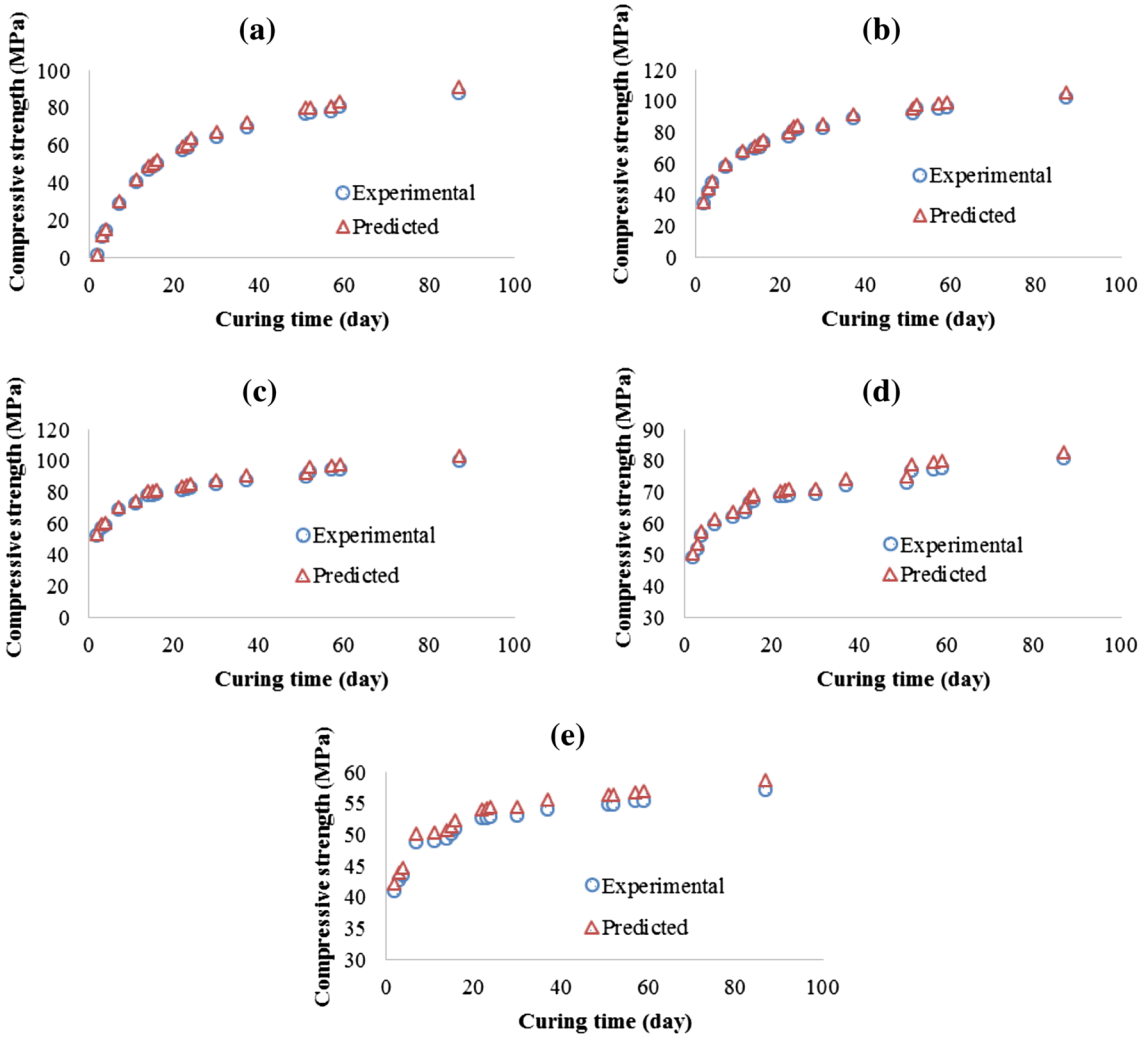

Fig. 4 Comparison of experimental results and predicted ones by the proposed model at temperatures of **a** 25 °C, **b** 45 °C, **c** 65 °C, **d** 85 °C, and **e** 100 °C

Table 7 Values of α and β for all curing temperature used in this study

Curing temperature (°C)	α	β
25	0.5495	1.4556
45	0.4420	1.9349
65	0.2937	1.9441
85	0.1978	1.5880
100	0.1104	1.2223

Table 8 Values of average relative errors of the model at curing temperatures used in this study

Curing temperature (°C)	Average error (%)
25	3.48
45	2.89
65	2.94
85	2.57
100	2.65

which both are dimensionless. Also, the model has two generalized parameters, α and β, among which the former is a linear function of dimensionless curing temperature and the latter is as a quadratic function of dimensionless curing temperature. The proposed model can easily predict the compressive strength of chemically activated high phosphorus slag content cement at different curing temperatures and times with an average error of less than 4%.

References

1. Khurana S, Banerjee R, Gaitonde U (2002) Energy balance and cogeneration for a cement plant. Appl Therm Eng 22:485–494
2. Hekal EE, Abo-El-Enein SA, El-Korashy SA, Megahed GM, El-Sayed TM (2013) Hydration characteristics of portland cement–electric arc furnace slag blends. HBRC J 9:118–124
3. Palaniappan KA, Vasantha S, Prakasan SS, Prabhu S, GGBS as alternative to OPC in concrete as an environment pollution reduction approach (2013) Int J Eng Res Technol 6(2):190–195
4. Kumar S, Kumar R, Bandopadhyay A, Innovative methodologies for the utilization of wastes from metallurgical and allied industries. Resour, Conserv Recycl, 2006; 48, 301–314.
5. Dongxu L, Xuenquan W, Jinlin S, Yujiang W (2000) The influence of compound admixtures on the properties of high-Content slag cement. Cem Concr Res 30:45–50
6. Kumar S., Kumar R., Bandopadhyay A., Alex T.C., Ravi Kumar B., Das S.K., Mehrotra S.P. (2008)Mechanical activation of granulated blast furnace slag and its effect on the properties and structure of portland slag cement. Cem Concr Compos, ; 30, 679–685.
7. Xia C, Li Z, Kunhe F (2009) Anti-crack performance of phosphorus slag concrete. Wuhan Univ J Nat Sci 1(14):80–86
8. Xia C, Kunhe F, Huaquan Y, Hua P (2011) Hydration kinetics of phosphorous slag-cement paste.Wuhan Univ J Nat Sci 1(26):142–146
9. Lothenbach B, Scrivener K, Hooton R (2011) Supplementary cementitious materials. Cem Concr Res 41:1244–1256
10. Scrivener K, Nonat A (2011) Hydration of cementitious materials, present and future. Cem Concr Res 41(7):651–665
11. Allahverdi A, Shaverdi B, Najafi Kani E (2010) Influence of sodium oxide on properties of fresh and hardened paste of alkali-activated blast-furnace slag. Int J Civ Eng 8(4):304–314
12. Ben Haha M, Lothenbach B, Le Saout G, Winnefeld F (2012) Influence of slag chemistry on the hydration of alkali-activated blast-furnace slag-part II: effect of Al_2O_3. Cem Concr Res 42:74–83
13. Chen L (2010) A multiple linear regression prediction of concrete compressive strength based on physical properties of electric arc furnace oxidizing slag. Int J Appl Sci Eng 2(7):153–158
14. Dongxu L, Xuenquan W, Jinlin S Yujiang W (2002) A blended cement containing blast furnace slag and phosphorous slag. J Wuhan Univ Technol 2(17):62–65
15. Dong XL, Lin C, Zhong-zi X, Zhi-min L (2002) A blended cement containing blast furnace slag and phosphorous slag. J Wuhan Univ Technol 2(17):62–65
16. Allahverdi A, Saffari M (2011) Chemical activation of phosphorous slag with a solid compound activator, In: Proceedings of 4th International Conference on non-traditional cements and concretes. Brno, Czech Republic 573–580
17. Allahverdi A, Rahmani A (2009) Chemical activation of natural pozzolan with a solid compound activator. Cem Wapno Beton 4:205–213
18. Allahverdi A, Ghorbani J (2006) Chemical activation and set acceleration of lime-natural pozzolan cement. Ceram Silik 50:193–199
19. Tepecik A, Altin Z, Erturan S (2009) Modeling compressive strength of standard cem-i 42.5 cement produced in Turkey with stepwise regression method. J Chem Soc Pak 2(31):214–220
20. Chopra P, Sharma RK, Kumar M (2014) Regression models for the prediction of compressive strength of concrete with & without fly ash. Int J Latest Trends Eng Technol 4(3):400–406
21. Iqbal Khan M (2009) Analytical model for the strength prediction of hpc consisting of cementitious composites Archit Civ Eng Environ 1:89–96
22. Eswari S, Raghunath PN, Kothandaraman S (2011) Regression modeling for strength and toughness evaluation of hybrid fibre reinforced concrete, ARPN J Eng Appl Sci 5 (6), 1–8
23. Onal O, Oztutk AU (2010) Artificial neural network application on microstructure-compressive strength relationship of cement mortar. Adv Eng Software 41:165–169
24. Akkurt S, Ozdemir S, Tayfur G, Akyol B (2003) The use of GA-ANNs in the modeling of compressive strength of cement mortar. Cem Concr Res 33:973–979
25. Saridemir M (2009) Prediction of compressive strength of concretes containing metakaolin and silica fume by artificial neural networks. Adv Eng Softw 40:350–355
26. Oztas A, Pala M, Eozbay E, Kanca E, Cag Iar N, Asghar M (2006) Prediction the compressive strength and slump of high strength concrete using neural network. Constr Build Mater 20:769–775
27. Saridemir M (2010) Genetic programming approach for prediction of compressive strength of concretes containing rice husk ash. Constr Build Mater 24:1911–1919
28. Ahmadi M, Naderpour H, Kheyroddin A, ANN model for predicting the compressive strength of circular steel-confined concrete., Int J Civ Eng. doi:10.1007/s40999-016-0096-0

29. Tarighat A (2012) Stochastic modeling and calibration of chloride content profile in concrete based on limited available data. Int J Civ Eng 4(10):309–316
30. Kenai S., Bhalerao K.D., Soboyejo A.B.O., Soboyejo W.O. (2006) A stochastic model for strength of limestone concrete, .
31. Christensen P.T., Stochastic modeling of the diffusion coefficient for concrete, In: Proceedings of IFIP Working Conference, Osaka, Japan, 2002
32. Hariharan AR, Santhi AS, Mohan Ganesh G (2015) Statistical model to predict the mechanical properties of binary and ternary blended concrete using regression analysis. Int J Civ Eng Trans A 13(3):331–340
33. Silvestri S, Gasparini G, Trombetti T, Ceccoli C, Statistical analysis towards the identification of accurate probability distribution models for the compressive strength of concrete, In: Proceedings of the 14th World Conference on Earthquake Engineering. Beijing, China, 2008
34. Chopra P, Sharma RK, Kumar M (2013) Ridge regression for the prediction of compressive strength of concrete. Int J Innov Eng Technol 3(2):106–111
35. Allahverdi A, Mahinroosta M (2014) A model for prediction of compressive strength of chemically activated high phosphorous slag content cement. Int J Civ Eng Trans A 4(12):481–487